Myeloproliferative Disease in Mice with Reduced Presenilin Gene Dosage: Effect of γ-Secretase Blockage[†]

Yibing Qyang,[‡] Stuart M. Chambers,[§,||] Pei Wang,[‡] Xuefeng Xia,[‡] Xiaoli Chen,[‡] Margaret A. Goodell,[§,||,⊥] and Hui Zheng*[,‡,§,⊥]

Huffington Center on Aging, Interdepartmental Program in Cellular and Molecular Biology, Center for Cell and Gene Therapy, and Department of Molecular and Human Genetics, Baylor College of Medicine, Houston, Texas 77030

Received January 23, 2004; Revised Manuscript Received March 1, 2004

ABSTRACT: Mammalian presenilins (PS) consist of two highly homologous proteins, PS1 and PS2. Because of their indispensable activity in the γ-secretase cleavage of amyloid precursor protein to generate Aβ peptides, inhibition of PS γ-secretase activity is considered a potential therapy for Aβ blockage and Alzheimer's disease intervention. However, a variety of other substrates are also subject to PS-dependent processing, and it is thus imperative to understand the consequences of PS inactivation in vivo. Here we report a pivotal role of PS in hematopoiesis. Mice heterozygous for *PS1* and homozygous for *PS2* ($PS1^{+/-}PS2^{-/-}$) developed splenomegaly with severe granulocyte infiltration. This was preceded by an overrepresentation of granulocytic cells in the bone marrow and a greatly increased multipotent granulocyte−monocyte progenitor in the spleen. In contrast, hematopoietic stem cells and T- and B-lymphocytes were not affected. Importantly, treatment of wild-type splenocytes with a γ-secretase inhibitor directly promoted the granulocyte−macrophage colony-forming unit (GM-CFU). These results establish a critical role of PS in myelopoiesis. Our finding that this activity can be directly modulated by its γ-secretase activity has important safety implications concerning these inhibitors.

Alzheimer's disease (AD) is the most common form of senile dementia characterized by the deposition of β-amyloid plaques in specific areas of the brain. The major components of the plaques are 40−42 amino acid peptides referred to as Aβ[1] that are derived by proteolytic cleavages of the amyloid precursor protein (APP) (reviewed in ref *1*). Mutations in presenilin genes (*PS1* and *PS2*) lead to dominant inheritance of early onset of familial AD, and these mutations are known to affect the γ-secretase cleavage of APP and to foster the amyloid plaque pathology (*1*). Indeed, PS have been shown to be absolutely required for the γ-secretase activity to generate Aβ peptides: Inactivation of PS1 results in an 80% reduction of Aβ (*2*), and a complete inhibition is achieved in cells lacking both PS1 and PS2 (*3*, *4*). Pharmacologically, γ-secretase inhibitors have been developed to block Aβ production, and these inhibitors are known to target presenilins (*5*).

APP, however, is not the sole substrate of PS. Through similar mechanisms defined as regulated intramembrane proteolysis (RIP) (*6*), PS have been reported to process numerous other proteins, mostly noticeably Notch (*7*), molecules that regulate various cell-fate specification processes. In mammalian systems, the two presenilins play compensatory roles as revealed by gene knockout studies. Specifically, *PS1* null mice die perinatally, exhibiting a partial Notch-associated somite segmentation defect (*8*, *9*). While the *PS2* knockout does not lead to overt impairment, *PS1* and *PS2* double null embryos die during early embryonic development, exhibiting a complete *Notch* loss-of-function phenotype (*10*, *11*). Thus, a defective Notch processing and signaling are likely to account for the developmental phenotypes of PS null animals.

Hematopoiesis is a complex process by which self-renewing hematopoietic stem cells (HSC) in the bone marrow give rise to common lymphoid progenitors (CLP) and common myeloid progenitors (CMP). CLP differentiate into precursors of T- and B-lymphocytes, while CMP give rise to megakaryocyte−erythrocyte progenitors (MEP) and granulocyte−monocyte progenitors (GMP), which will further develop to platelets and erythrocytes and granulocytic (neutrophil, eosinophil, and basophil) and monocytic cells, respectively (reviewed in ref *12*). Members of the Notch receptors and ligands are expressed in various cell types of developing and adult hematopoietic systems, and evidence has been presented for their role in the survival, proliferation, and differentiation of HSC and multiple progenitor and precursor cells (reviewed by ref *13*). However, in contrast

[†] This work was supported by grants from the NIH (NS40039 and AG20670) and the Alzheimer's Association (IIRG-00-2221). H.Z. is a New Scholar of the Ellison Medical Foundation and M.A.G. is a scholar of the Leukemia and Lymphoma Society.

* Corresponding author. Phone: 713-798-1568. Fax: 713-798-1610. E-mail: huiz@bcm.tmc.edu.

[‡] Huffington Center on Aging.

[§] Interdepartmental Program in Cellular and Molecular Biology.

[||] Center for Cell and Gene Therapy.

[⊥] Department of Molecular and Human Genetics.

[1] Abbreviations: PS, presenilins; Aβ, β-amyloid peptides; GM-CFU, granulocyte−macrophage colony-forming unit; HSC, hematopoietic stem cells; CLP, common lymphoid progenitors; CMP, common myeloid progenitors; MEP, megakaryocyte−erythrocyte progenitors.

10.1021/bi049826u CCC: $27.50
Published on Web 04/10/2004

to its well-documented activity in T- and B-lineage commitment, most of the studies concerning the role of the Notch signaling pathway in myeloid lineage employed gain-of-function studies in cell culture systems, and conflicting data have been reported (*14*, *15*). Furthermore, a link between Notch1 and myeloid development could not be established in vivo (*16*).

Although *PS1*-deficient mice are embryonic lethal (*8*, *9*), *PS2* null ($PS2^{-/-}$) and *PS1* heterozygous ($PS1^{+/-}$) mice are viable on both individual or combined (i.e., $PS1^{+/-}PS2^{-/-}$) background (*10*). We report here that mice with reduced presenilin dosage develop an age-dependent myeloproliferative disease, and we propose that it is mediated through its γ-secretase activity.

EXPERIMENTAL PROCEDURES

Mice and Reagents. The generation and genotyping of *PS1* and *PS2* null mice have previously been described (*9*, *10*). They were housed in a SPF facility. All procedures were performed in accordance with the Baylor College of Medicine Institutional Animal Care and Use Committee and the National Institutes of Health guidelines.

Antibodies used for HSC and FACS analyses were obtained from PharMingen. Anti-cyclin D1 and MPO antibodies were from Santa Cruz and DAKO, respectively.

Histological Methods. Tissues were fixed in 10% neutral buffered formalin for 24−48 h, dehydrated through graded alcohols, and stored in 70% ethanol at 4 °C. Tissues were vacuum-embedded in paraffin, sectioned at 5 μm, and stained with hematoxylin and eosin.

Peripheral blood was collected by retroorbital bleeding. The blood smear was stained with Wright−Giemsa solutions (Fluka). Total and differential blood counts were determined using an automated H-1 analyzer (Technicon Instruments Corp.).

Flow Cytometry. Cells were resuspended at 1×10^6 per 100 μL of PBS containing 2% FCS and 1 μg of mouse Fcγ III/II receptor antibody for 10 min and then stained for 20 min at 4 °C with the indicated mouse antibodies (PharMingen). For spleen cells, 5 mL of RBC lysis buffer (9 volumes of 0.16 M NH_4Cl + 1 volume of 0.17 M Tris-HCl, pH 7.65) was added, and cells were incubated at room temperature for 5 min followed by washing two times in PBS + 2% FCS. Viable cells, gated by light scatter, were sorted and analyzed on a FACSCalibur cell sorter using CellQuest software (Becton Dickinson). The Gr-1/annexin V double labeling was performed as described (*17*).

Hematopoietic Stem Cell Analysis. Bone marrow was flushed from the tibias and femurs of WT, $PS2^{-/-}$, and $PS1^{+/-}PS2^{-/-}$ mice. The marrow was resuspended at 10^6 cells/mL in DMEM containing 2% FCS (Hyclone) and 10 mM HEPES buffer (Life Technologies). The cells were then stained with 5 μg/mL Hoechst 33342 (Sigma-Aldrich) for 90 min at 37 °C, as described previously (*18*), and then resuspended in cold HBSS supplemented with 2% FCS, 10 mM HEPES, and 2 μg/mL propidium iodide. Analysis of SP cells was performed on a triple-laser instrument (MoFlow; Cytomation Inc., Fort Collins, CO).

Spleen GM-CFU Assay. Primary splenocytes (5×10^5) were resuspended in 0.6 mL of DMEM supplemented with 2% fetal bovine serum. MethoCult TM M3234 medium (2.4 mL) (StemCell Technologies) containing GM-CSF (5.3 ng/mL, PeproTech Inc.) was added, mixed thoroughly, and plated to two 35 × 10 mm Petri dishes. When the γ-secretase inhibitor effect was tested, a final concentration of 0.5 μM drug was added to the medium, and the same amount of DMSO without compound was added to a separate dish as vehicle control. Cells were cultured in a 37 °C incubator maintained with 5% CO_2 and 95% humidity. Colonies were counted after 7−8 days under a light microscope.

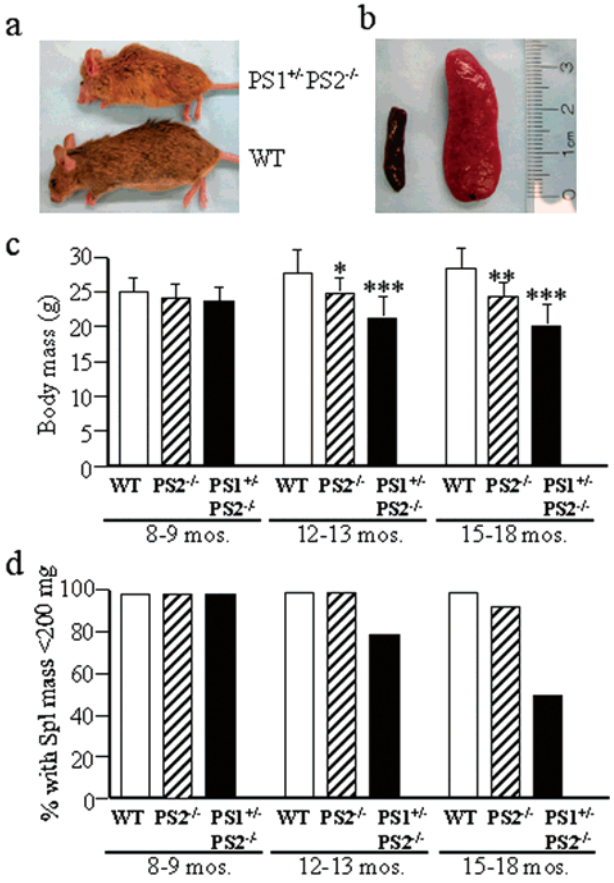

FIGURE 1: Morphological characterization of presenilin mutant mice. (a) A representative 18-month-old $PS1^{+/-}PS2^{-/-}$ animal (top) showing reduced body size and kyphosis. The lower panel is an age-matched wild-type (WT) control. (b) Splenomegaly in the $PS1^{+/-}PS2^{-/-}$ mutant (right) with a wild-type spleen shown on the left. (c) Mean body mass (grams) of female WT, $PS2^{-/-}$, and $PS1^{+/-}PS2^{-/-}$ animals at 8−9, 12−13, and 15−18 months of age (N = 20/group). Numbers shown are the average ± SD. Key: *, $P < 0.05$; **, $P < 0.01$; ***, $P < 0.001$; Student's t-test. (d) Percentage of mice (males and females) that do not show splenomegaly (spleen mass <200 mg). N = 20/group for 8−9 month old and N = 40/group for 12−13 and 15−18 month old animals, respectively.

RESULTS

Morphological and Histological Characterization of $PS2^{-/-}$ and $PS1^{+/-}PS2^{-/-}$ Mice. The $PS2^{-/-}$ and $PS1^{+/-}PS2^{-/-}$ mice were generated by crossing the $PS1^{+/-}PS2^{-/-}$ males with $PS2^{-/-}$ females and were of mixed C57/129Sv background. These animals, along with their age- and strain-matched wild-type controls, were housed in a specific pathogen-free (SPF) environment. All animals were overtly healthy at a young age. However, from approximately 1 year of age and onward, the $PS1^{+/-}PS2^{-/-}$ mice showed progressive reduction of body mass, kyphosis, and loss of vigor (Figure 1a). Post-mortem

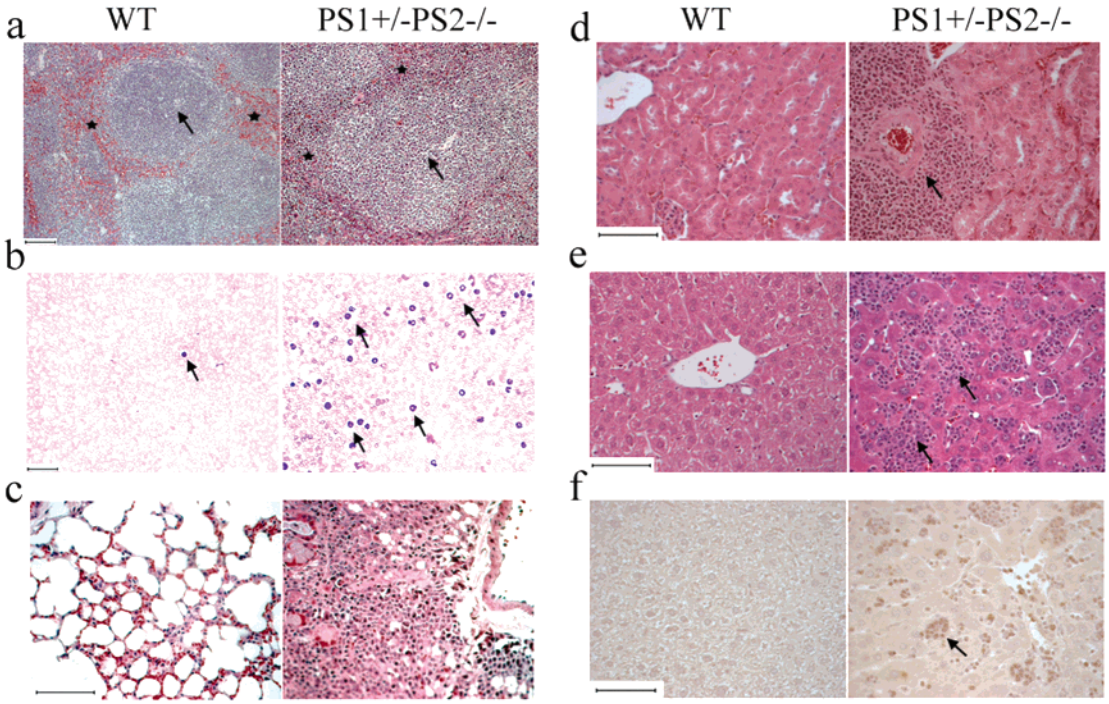

FIGURE 2: Histological analysis of diseased 18-month-old $PS1^{+/-}PS2^{-/-}$ animals (right) as compared with their corresponding age-matched wild-type controls (left). (a) H and E staining of spleen sections. Key: arrows, white pulp; stars, red pulp. (b) Wright−Giemsa staining of blood smear, documenting greatly elevated dark-stained granulocytic cells in $PS1^{+/-}PS2^{-/-}$ mutants (arrows). (c−e) Granulocytic infiltration into lung (c), kidney (d), and liver (e). Arrows denote infiltrated cells. (f) Positive MPO staining (arrow) in liver of $PS1^{+/-}PS2^{-/-}$ mice. Scale bar = 50 μM.

Table 1: Hematological Parameters of $PS2^{-/-}$ and $PS1^{+/-}PS2^{-/-}$ Mice[a]

	8−9 months			12−13 months			15−18 months			
									$PS1^{+/-}PS2^{-/-}$	
parameter	WT	$PS2^{-/-}$	$PS1^{+/-}PS2^{-/-}$	WT	$PS2^{-/-}$	$PS1^{+/-}PS2^{-/-}$	WT	$PS2^{-/-}$	healthy	diseased
Spl mass (mg)	100 ± 80	65 ± 15	75 ± 12	89 ± 24	73 ± 14	74 ± 21	83 ± 26	80 ± 17	127 ± 42	590 ± 420[c]
leukocytes ($\times 10^3/\mu$L)	5.2 ± 1.9	5.7 ± 2.7	8.3 ± 2.1	4.7 ± 1.5	8.9 ± 4.8	**9.9 ± 4.4**[b]	3.1 ± 0.5	**11 ± 4**[c]	**14 ± 2**[c]	**46 ± 23**[c]
erythrocytes ($\times 10^6/\mu$L)	9.2 ± 0.7	8.9 ± 0.6	9.1 ± 0.4	9.4 ± 0.3	8.8 ± 0.4	8.9 ± 0.6	9.1 ± 0.4	8.8 ± 0.5	7.0 ± 1.8	6.4 ± 1.4[c]
platelets ($\times 10^6/\mu$L)	1.1 ± 0.3	1.1 ± 0.3	1.3 ± 0.2	1.1 ± 0.3	1.5 ± 0.3	1.7 ± 0.3	1.1 ± 0.2	1.7 ± 0.4	1.6 ± 0.4	1.3 ± 0.3
Neut (%)	13 ± 4	21 ± 9	**22 ± 5**[b]	17 ± 4	20 ± 7	**26 ± 7**[b]	18 ± 4	33 ± 21	**36 ± 15**[b]	**47 ± 8**[c]
Lymp (%)	78 ± 3	72 ± 7	70 ± 6[b]	72 ± 6	70 ± 8	63 ± 9[b]	72 ± 6	56 ± 20	51 ± 17[b]	22 ± 14[c]
Mono (%)	5.6 ± 2.6	3.9 ± 0.1	4.5 ± 1.0	7.0 ± 2.0	4.8 ± 0.9	4.8 ± 0.8	6.0 ± 0.8	6.8 ± 2.8	4.6 ± 0.8[b]	3.1 ± 1.7[b]
Eos (%)	1.7 ± 1.2	1.8 ± 1.6	2.3 ± 1.4	2.4 ± 0.9	3.3 ± 1.3	4.0 ± 2.5	2.0 ± 0.8	2.1 ± 1.5	**5.4 ± 1.7**[b]	**22 ± 13**[c]

[a] Peripheral blood was collected from wild-type (WT), $PS2^{-/-}$, and $PS1^{+/-}PS2^{-/-}$ mice at 8−9, 12−13, and 15−18 months of age, respectively, by retroorbital bleeding. The 15−18 month old $PS1^{+/-}PS2^{-/-}$ animals were subdivided into two groups: those morphologically indistinguishable from the wild-type control (healthy) and those that appeared sick and exhibited splenomegaly (diseased). Total (leukocytes, erythrocytes, and platelets) and differential (neutrophils, lympocytes, monocytes, and eosinophils) blood counts were determined using an automated H-1 analyzer. Results are the mean ± SD. $N = 5-8$ mice/group. Abbreviations: Spl, spleen; Neut, neutrophil; Lymp, lymphocyte; Mono, monocyte; Eos, eosinophil. Leukocytic cells that are significantly altered are shown in bold. [b] $P < 0.05$. [c] $P < 0.001$.

analysis revealed profoundly enlarged spleen (Figure 1b) and lymph nodes (not shown). Longitudinal followup of a cohort of 100 mice/genotype documented that, at 8−9 months, the body weight and the spleen mass of $PS2^{-/-}$ and $PS1^{+/-}PS2^{-/-}$ mice were comparable with the wild-type controls (Figure 1c,d). However, both the $PS2^{-/-}$ and $PS1^{+/-}PS2^{-/-}$ animals had reduced body mass at 1 year of age, and this difference became more dramatic at 15−18 months (Figure 1c). Mice heterozygous for PS1 alone ($PS1^{+/-}PS2^{+/+}$) were apparently not affected (not shown). Measurement of spleen mass showed that while splenomegaly (defined as spleen mass >200 mg) was rare among *PS2* null, 20% of the $PS1^{+/-}PS2^{-/-}$ animals exhibited splenomegaly at 1 year of age, and this number increased to 50% at 15−18 months (Figure 1d). Mice with splenomegaly were invariably under weight and were termed "diseased".

H and E analysis of diseased spleen documented the presence of recognizable red pulp (stars) and white pulp (arrow) structures (Figure 2a, right). However, compared to the normal spleen (left), these structures were less well defined. Wright−Giemsa staining of peripheral blood of diseased animals revealed greatly elevated mature leukocytes (Figure 2b, arrows). This was accompanied by severe infiltration of granulocytic cells into peripheral tissues such

as lung (Figure 2c), kidney (Figure 2d), and liver (Figure 2e). Although the infiltrated cells were predominately of mature type, immature cells positive for myeloperoxidase (MPO) could be identified in mice with severe splenomegaly (spleen mass >1000 mg) (Figure 2f). Modified Steiner's stain did not reveal any evidence of argyrophilic helical bacteria (data not shown), arguing against the possibility that elevated granulocytic cells were the result of infection.

Hematological Evaluation of PS2$^{-/-}$ and PS1$^{+/-}$PS2$^{-/-}$ Animals. We characterized the hematological profiles of PS animals by performing both total and differential blood counts. Analysis of diseased PS1$^{+/-}$PS2$^{-/-}$ animals revealed markedly elevated leukocytes and percentages of granulocytic cells, including neutrophils and eosinophils (Table 1, far right column, with numbers highlighted in bold). This was accompanied by a significant reduction in the number of erythrocytes and percentages of lymphocytes and monocytes. Interestingly, the hematological abnormality was not limited to diseased animals. Analysis of healthy PS1$^{+/-}$PS2$^{-/-}$ mice at 8−9, 12−13, and 15−18 months documented an age-dependent increase in both the total number of leukocytes and the percentage of leukocytic neutrophils (Table 1, with numbers shown in bold). The PS2$^{-/-}$ animals exhibited similar trends, although statistically significant differences often cannot be reached due to large individual variations (Table 1). As myeloid hyperplasia was age-dependent and preceded overt clinical phenotype, our result again suggests that increased granulocytes were caused by an intrinsic hematopoietic defect rather than secondary to infection.

Lineage Analysis of Presenilins in Hematopoiesis. To further provide experimental evidence for a primary effect of presenilins in granulocytic lineage, we performed fluorescence-activated cell sorter (FACS) analysis of bone marrow and spleen cells isolated from healthy animals at 6−8, 9, and 12−13 months of age, respectively (Figure 3). Quantification of Gr-1^{hi}/Mac-1^{hi} granulocytic cells in the bone marrow (Figure 3a) and spleen (Figure 3b) revealed a normal percentage of Gr-1^{hi}/Mac-1^{hi} cells at 6−8 months. However, this ratio was already significantly increased in the splenocytes of PS1$^{+/-}$PS2$^{-/-}$ mice at 9 months (Figure 3b). Although an increase was also observed in the bone marrow of these mice (Figure 3a) and in the spleen of *PS2* null (Figure 3b) at this age, the differences failed to reach statistical significance. At 12−13 months, the percentage of Gr-1^{hi}/Mac-1^{hi} cells was significantly elevated in both the bone marrow and spleen of PS2$^{-/-}$ and PS1$^{+/-}$PS2$^{-/-}$ animals (Figure 3a−c).

Since the Notch pathway and the presenilins have been shown to regulate lymphopoiesis and T-cell development (*19*−*21*), we measured T-cell profiles in the spleen and thymus by surface labeling with anti-CD4 and -CD8 antibodies (Figure 4a). Likewise, B-cells in the spleen and bone marrow were evaluated for their expression of IgM and CD19 (Figure 4b). The results documented that neither T- nor B-lymphocytes were significantly altered in the presenilin mutants. These data thus indicate that reduced presenilins specifically affect the myeloid lineage.

As hematopoiesis initiates from the hematopoietic stem cells (HSC), and the Notch pathway molecules have been implicated in the maintenance and survival of HSC (*22*, *23*), it could be argued that presenilins may affect HSC through

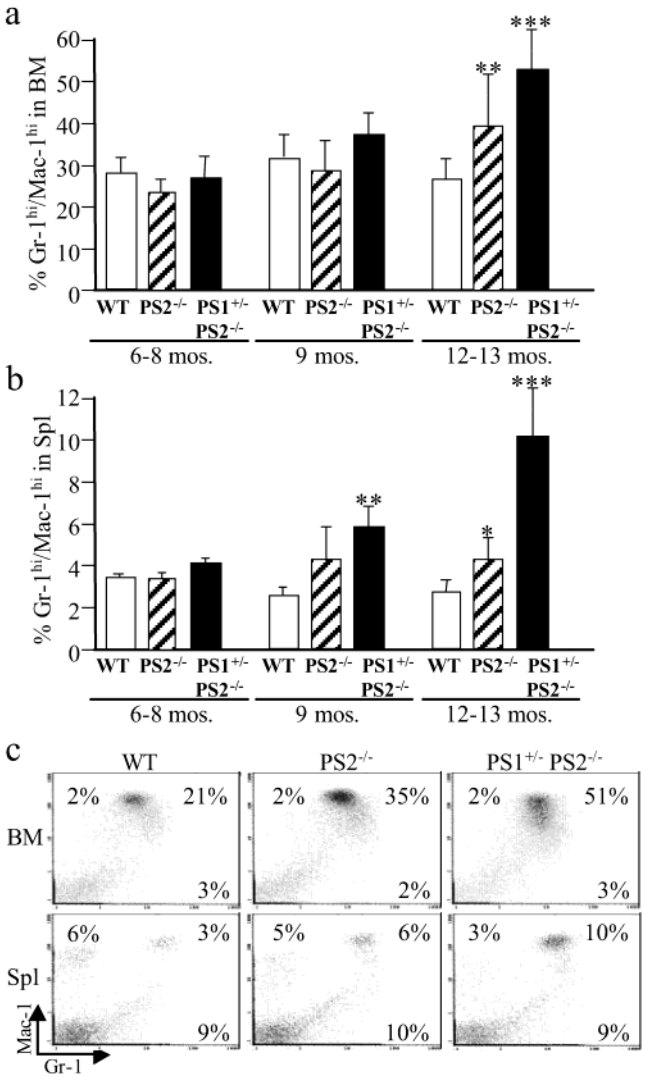

FIGURE 3: Flow cytometric analysis of Gr-1/Mac-1 lineage. (a, b) Percentage of Gr-1^{hi}/Mac-1^{hi} granulocytes in bone marrow (BM, panel a) and spleen (Spl, panel b) of 6−8, 9, and 12−13 month old healthy WT (N = 5/group), PS2$^{-/-}$ (N = 15/group), and PS1$^{+/-}$PS2$^{-/-}$ (N = 15/group) animals, respectively. Numbers shown are the average ± SD. Key: *, $P < 0.05$; **, $P < 0.01$; ***, $P < 0.001$; Student's t-test. (c) Representative Gr-1/Mac-1 profiles in bone marrow (BM) and spleen (Spl) of 12-month-old animals.

the Notch signaling pathway, which in turn leads to impaired myeloid lineage. To explore this mechanism, we measured the number of HSC as a function of presenilin gene dosage using the Hoechst dye efflux assay. This assay relies on the property that primitive HSC are capable of effluxing the fluorescent dye Hoechst 33342 and can be highly enriched from a side population (SP) (*18*). Quantification of bone marrow HSC in 2-, 9-, and 12-month-old PS2$^{-/-}$ and PS1$^{+/-}$PS2$^{-/-}$ mice did not identify any appreciable differences when compared with that of the wild-type animals (Figure 4c).

Having documented that the number of HSC was not altered in presenilin mutant animals, we next examined the multipotent granulocyte−monocyte progenitors (GMP) using an in vitro colony-forming assay. Quantification of the splenocyte-derived granulocyte−macrophage colony-forming unit (GM-CFU) of 1-year-old mice revealed a 7−8-fold increase in PS1$^{+/-}$PS2$^{-/-}$ samples compared with that

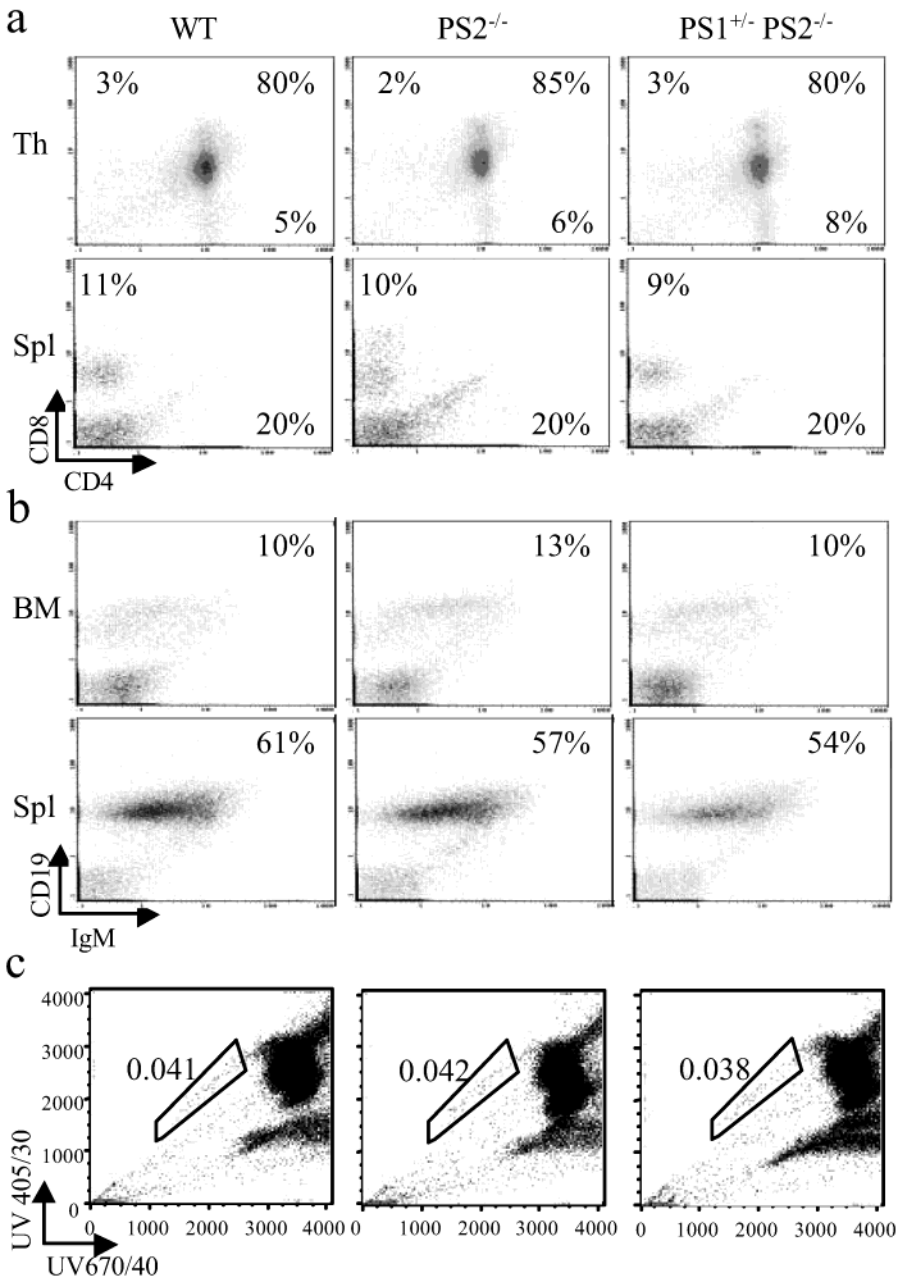

FIGURE 4: Similar T-cell (a), B-cell (b), and HSC (c) profiles in 12-month-old WT, $PS2^{-/-}$, and $PS1^{+/-}PS2^{-/-}$ animals: (a) CD4/CD8 in thymus (Th) and spleen (Spl); (b) IgM/CD19 in bone marrow (BM) and spleen (Spl); (c) representative side-population (SP) profiles. Numbers shown are the percentage of SP cells within the nucleated cells of whole bone marrow.

of wild-type controls (Figure 5a). These data were indicative of extramedullary hematopoiesis in the presenilin mutant.

We reported that loss of PS1 in skin results in epidermal hyperproliferation and cyclin D1 activation (*24*). To investigate whether this is the mechanism contributing to increased spleen GM-CFU, we measured cyclin D1 levels by western blot analysis. The results showed an invariable increase of cyclin D1 in multiple $PS1^{+/-}PS2^{-/-}$ samples (Figure 5b). To evaluate whether a reduced apoptosis may also be responsible for enhanced GM-CFU, we determined the granulocytic cells undergoing apoptosis by quantifying the percentage of Gr-1 and annexin V double positive cells by FACS analysis (Figure 5c). No significant differences were observed between the controls and presenilin mutants. These data combined suggest that an accelerated cell proliferation is the underlying mechanism for the dramatic increase of GM-CFU in $PS1^{+/-}PS2^{-/-}$ splenocytes.

γ-Secretase Inhibitor Promotes GM-CFU. Taking advantage of the availability of γ-secretase inhibitors, we decided to directly assess the role of γ-secretase activity on the granulocyte−monocyte progenitor. A highly potent and specific inhibitor (compound 15) with a half-maximal inhibitory concentration (IC_{50}) of 1.2 nM was chosen (*25*).

Primary splenocytes isolated from 12-month-old wild-type animals were treated either with DMSO as vehicle control or with 0.5 μM inhibitor, and the number of GM-CFU was quantified after 7−8 days of culturing. Combination of three independent experiments revealed a 2.5-fold increase of GM-CFU in the presence of the γ-secretase inhibitor (Figure 5d). In addition to the absolute numbers, we also noticed that the colony size was larger in the inhibitor-treated cultures

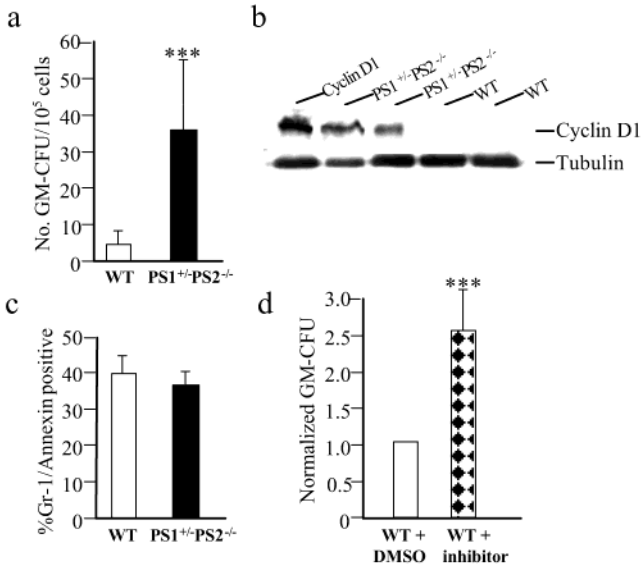

FIGURE 5: Effect of presenilins on GM-CFU. (a) Average number of GM-CFU (mean ± SD) per 10^5 cells in WT and $PS1^{+/-}PS2^{-/-}$ splenocytes. Key: ***, $P < 0.001$; Student's *t*-test. (b) Corresponding cyclin D1 activation in the spleen samples of $PS1^{+/-}PS2^{-/-}$ mice. Lane labeled as cyclin D1: CHO cells transfected with cyclin D1. β-Tubulin was used as loading control. (c) Percentage of Gr-1/annexin V double positive cells (mean ± SD) in 12-month-old WT, $PS2^{-/-}$, and $PS1^{+/-}PS2^{-/-}$ splenocytes. (d) Fold increase of GM-CFU in wild-type splenocytes treated with 0.5 μM γ-secretase inhibitor (WT + inhibitor) as compared with the vehicle control (WT + DMSO). Numbers shown are the relative fold increase ± SD of three independent experiments. Key: ***, $P < 0.001$; Student's *t*-test.

(not shown). This result thus supports a direct effect of presenilins on the proliferation of GMP. Similar results were obtained with another γ-secretase inhibitor DAPT (*26*).

DISCUSSION

We report in this study that partial loss of presenilins in mice leads to an age-dependent myeloproliferative disease. We showed that reduced presenilin dosage does not impair HSC. We performed multiple lines of analysis on hematopoietic cells in the bone marrow, peripheral blood, and spleen, and our data support the notion that the primary effect of presenilins is on cells of the granulocytic lineage, and the changes of these cells trigger the alterations of other cell types such as lymphocytes. Within the myeloid lineage, megakaryocyte−erythrocyte progenitors (MEP) are not likely affected, as we detected normal numbers of platelets and erythrocytes. However, presenilins play a pivotal role in the granulocyte−monocyte lineage since reduced presenilin expression in vivo and γ-secretase inhibitor treatment in vitro both lead to deregulation of granulocyte−monocyte progenitors (GMP). Elevated GMP in presenilin mutant animals is accompanied by an overrepresentation of $Gr\text{-}1^{hi}/Mac\text{-}1^{hi}$ population and an increased number of mature granulocytic cells. Therefore, granulocyte maturation does not require presenilins.

Our results support a model whereby presenilins primarily act to control the number of GMP at a late stage of hematopoiesis (Figure 6). This is in contrast to the vast amount of published reports implicating a widespread role of presenilin-dependent Notch signaling in the survival,

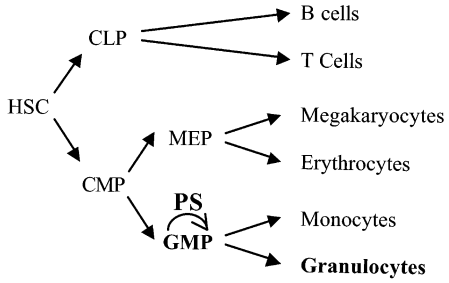

FIGURE 6: Proposed model of presenilins in hematopoiesis. The primary effect of presenilins (PS) is in the homeostasis of granulocyte−monocyte progenitors (GMP) through its γ-secretase activity. Inhibition or reduction of PS leads to increased GMP and overrepresentation of mature granulocytic cells. Other hematopoietic lineages, including hematopoietic stem cells (HSC), common lymphoid progenitors (CLP), common myeloid progenitors (CMP), or megakaryocyte−erythrocyte progenitors (MEP), are not directly affected but may be altered as a result of imbalance of the hematopoietic system.

proliferation, and differentiation of HSC and multiple progenitor and precursor cells (*13*). This could be explained by the fact that presenilins are only partially reduced in our animals. A comprehensive assessment of presenilins in hematopoiesis waits for the conditional knockout in which a complete inactivation of presenilins in the bone marrow can be achieved. Nevertheless, our results highlight a potent regulation of presenilins on GMP and demonstrate that the hematopoietic phenotypes of the $PS2^{-/-}$ and $PS1^{+/-}PS2^{-/-}$ mice were not caused by a disruption of HSC or early progenitors. Our data are also in line with the report that Notch is not required for the maintenance of HSC or the development of myeloid lineages (*16*).

It can be argued that elevated granulocytic cells in the circulating blood and peripheral tissues seen in our $PS2^{-/-}$ and $PS1^{+/-}PS2^{-/-}$ mice could be caused by infection rather than an intrinsic hematopoietic defect. The following evidence makes this interpretation highly unlikely: (1) the mice were housed in a SPF facility and staining of diseased tissues failed to detect any evidence of argyrophilic helical bacteria, (2) overrepresentation of $Gr\text{-}1^{hi}/Mac\text{-}1^{hi}$ granulocytes in bone marrow and spleen is an early event and precedes overt clinical phenotypes (changes in body weight and spleen mass), and (3) importantly, treatment of wild-type splenocytes with a γ-secretase inhibitor directly promotes GM-CFU.

While we have shown a clear regulation of presenilins in granulocyte homeostasis and that this effect is likely mediated through its γ-secretase activity, the molecular pathway regulating this activity remains to be established. This issue is complicated because while Notch is an obvious candidate, numerous other proteins have been reported to be substrates for presenilin-dependent proteolysis (reviewed in ref *27*). Although the physiological significance is not known, impaired processing of these molecules cannot be excluded as potential mechanisms for the myeloproliferative defects. We reported that loss of PS1 in mouse skin is associated with enhanced β-catenin signaling, activation of its downstream target cyclin D1, and epidermal neoplasia (*24*). This effect could be executed through both processing-independent mechanisms (*28*) or indirectly through Notch as loss of Notch1 has been shown to lead to enhanced β-catenin signaling (*29*). Therefore, it is conceivable that deregulation

of the β-catenin pathway may contribute to the myeloproliferative phenotype. Our finding that cyclin D1 levels were elevated in $PS1^{+/-}PS2^{-/-}$ splenocytes supports this notion. In this regard, it is interesting to note that a similar skin phenotype has also been observed in a subset of $PS1^{+/-}PS2^{-/-}$ (but not $PS2^{-/-}$) animals over 1 year of age. Since the myeloproliferative phenotype is present in both strains and at an earlier onset, it is unlikely that the hematopoietic defect is indirectly caused by the skin lesions, although the two phenotypes may indeed be mediated by the same molecular mechanisms.

Since presenilins are absolutely required for Aβ production, inhibition of presenilin γ-secretase activity has been actively pursued as a potential strategy for AD treatment. It remains to be determined whether these inhibitors will lead to unacceptable side effects caused by simultaneous disruption of Notch or other presenilin-mediated pathways. Our results that mice with partial loss of presenilins develop severe hematopoietic defects and that inhibition of γ-secretase activity directly promotes myeloid progenitors caution for a possible adverse effect even with partial γ-secretase inhibition. The age-dependent effect in presenilin animals cautions for a particular vulnerability in aged population that these inhibitors are intended to target. It is important to note, however, that the dose of the inhibitor used in this study (0.5 μM) is significantly higher than that required for Aβ inhibition (*25*). Therefore, it is possible that a therapeutic window can be established to achieve effective Aβ suppression without affecting Notch or other presenilin targets. Nevertheless, our finding calls for a careful assessment of the dose and long-term effect of these inhibitors.

ACKNOWLEDGMENT

We are grateful to D. Beasley for expert technical support and Drs. M. Shearman and H. Lewis for the generous gift of the γ-secretase inhibitor. The authors thank many of our colleagues, including Drs. J. Liu, X. Han, B. Zheng, J. Belmont, C. Brayton, D. Jones, J. Zhang, and X. Wu, who provided valuable guidance throughout the course of the studies.

REFERENCES

1. Selkoe, D. J. (1998) The cell biology of beta-amyloid precursor protein and presenilin in Alzheimer's disease, *Trends Cell Biol. 8*, 447−453.
2. De Strooper, B., Saftig, P., Craessaerts, K., Vanderstichele, H., Guhde, G., Annaert, W., Von Figura, K., and Van Leuven, F. (1998) Deficiency of presenilin-1 inhibits the normal cleavage of amyloid precursor protein, *Nature 391*, 387−390.
3. Herreman, A., Serneels, L., Annaert, W., Collen, D., Schoonjans, L., and De Strooper, B. (2000) Total inactivation of gamma-secretase activity in presenilin-deficient embryonic stem cells, *Nat. Cell Biol. 2*, 461−462.
4. Zhang, Z., Nadeau, P., Song, W., Donoviel, D., Yuan, M., Bernstein, A., and Yankner, B. A. (2000) Presenilins are required for gamma-secretase cleavage of beta-APP and transmembrane cleavage of Notch-1, *Nat. Cell Biol. 2*, 463−465.
5. Li, Y. M., Xu, M., Lai, M. T., Huang, Q., Castro, J. L., DiMuzio-Mower, J., Harrison, T., Lellis, C., Nadin, A., Neduvelil, J. G., et al. (2000) Photoactivated gamma-secretase inhibitors directed to the active site covalently label presenilin 1, *Nature 405*, 689−694.
6. Brown, M. S., Ye, J., Rawson, R. B., and Goldstein, J. L. (2000) Regulated intramembrane proteolysis: a control mechanism conserved from bacteria to humans, *Cell 100*, 391−398.
7. De Strooper, B., Annaert, W., Cupers, P., Saftig, P., Craessaerts, K., Mumm, J. S., Schroeter, E. H., Schrijvers, V., Wolfe, M. S., Ray, W. J., et al. (1999) A presenilin-1-dependent gamma-secretase-like protease mediates release of Notch intracellular domain, *Nature 398*, 518−522.
8. Shen, J., Bronson, R. T., Chen, D. F., Xia, W., Selkoe, D. J., and Tonegawa, S. (1997) Skeletal and CNS defects in Presenilin-1-deficient mice, *Cell 89*, 629−639.
9. Wong, P. C., Zheng, H., Chen, H., Becher, M. W., Sirinathsinghji, D. J., Trumbauer, M. E., Chen, H. Y., Price, D. L., Van der Ploeg, L. H., and Sisodia, S. S. (1997) Presenilin 1 is required for Notch1 and DII1 expression in the paraxial mesoderm, *Nature 387*, 288−292.
10. Donoviel, D. B., Hadjantonakis, A. K., Ikeda, M., Zheng, H., Hyslop, P. S., and Bernstein, A. (1999) Mice lacking both presenilin genes exhibit early embryonic patterning defects, *Genes Dev. 13*, 2801−2810.
11. Herreman, A., Hartmann, D., Annaert, W., Saftig, P., Craessaerts, K., Serneels, L., Umans, L., Schrijvers, V., Checler, F., Vanderstichele, H., et al. (1999) Presenilin 2 deficiency causes a mild pulmonary phenotype and no changes in amyloid precursor protein processing but enhances the embryonic lethal phenotype of presenilin 1 deficiency, *Proc. Natl. Acad. Sci. U.S.A. 96*, 11872−11877.
12. Wagers, A. J., Christensen, J. L., and Weissman, I. L. (2002) Cell fate determination from stem cells, *Gene Ther. 9*, 606−612.
13. Ohishi, K., Katayama, N., Shiku, H., Varnum-Finney, B., and Bernstein, I. D. (2003) Notch signaling in hematopoiesis, *Semin. Cell Dev. Biol. 14*, 143−150.
14. Milner, L. A., Bigas, A., Kopan, R., Brashem-Stein, C., Bernstein, I. D., and Martin, D. I. (1996) Inhibition of granulocytic differentiation by mNotch1, *Proc. Natl. Acad. Sci. U.S.A. 93*, 13014−13019.
15. Schroeder, T., and Just, U. (2000) Notch signaling via RBP-J promotes myeloid differentiation, *EMBO J. 19*, 2558−2568.
16. Radtke, F., Ferrero, I., Wilson, A., Lees, R., Aguet, M., and MacDonald, H. R. (2000) Notch1 deficiency dissociates the intrathymic development of dendritic cells and T cells, *J. Exp. Med. 191*, 1085−1094.
17. Liu, F., Wu, H. Y., Wesselschmidt, R., Kornaga, T., and Link, D. C. (1996) Impaired production and increased apoptosis of neutrophils in granulocyte colony-stimulating factor receptor-deficient mice, *Immunity 5*, 491−501.
18. Goodell, M. A., Brose, K., Paradis, G., Conner, A. S., and Mulligan, R. C. (1996) Isolation and functional properties of murine hematopoietic stem cells that are replicating in vivo, *J. Exp. Med. 183*, 1797−1806.
19. MacDonald, H. R., Wilson, A., and Radtke, F. (2001) Notch1 and T-cell development: insights from conditional knockout mice, *Trends Immunol. 22*, 155−160.
20. Hadland, B. K., Manley, N. R., Su, D., Longmore, G. D., Moore, C. L., Wolfe, M. S., Schroeter, E. H., and Kopan, R. (2001) Gamma secretase inhibitors repress thymocyte development, *Proc. Natl. Acad. Sci. U.S.A. 98*, 7487−7491.
21. Doerfler, P., Shearman, M. S., and Perlmutter, R. M. (2001) Presenilin-dependent gamma-secretase activity modulates thymocyte development, *Proc. Natl. Acad. Sci. U.S.A. 98*, 9312−9317.
22. Varnum-Finney, B., Xu, L., Brashem-Stein, C., Nourigat, C., Flowers, D., Bakkour, S., Pear, W. S., and Bernstein, I. D. (2000) Pluripotent, cytokine-dependent, hematopoietic stem cells are immortalized by constitutive Notch1 signaling, *Nat. Med. 6*, 1278−1281.
23. Karanu, F. N., Murdoch, B., Miyabayashi, T., Ohno, M., Koremoto, M., Gallacher, L., Wu, D., Itoh, A., Sakano, S., and Bhatia, M. (2001) Human homologues of Delta-1 and Delta-4 function as mitogenic regulators of primitive human hematopoietic cells, *Blood 97*, 1960−1967.
24. Xia, X., Qian, S., Soriano, S., Wu, Y., Fletcher, A. M., Wang, X.-J., Koo, E. H., Wu, X., and Zheng, H. (2001) Loss of presenilin 1 is associated with enhanced beta-catenin signaling and skin tumorigenesis, *Proc. Natl. Acad. Sci. U.S.A. 98*, 10863−10868.
25. Churcher, I., Williams, S., Kerrad, S., Harrison, T., Castro, J. L., Shearman, M. S., Lewis, H. D., Clarke, E. E., Wrigley, J. D., Beher, D., et al. (2003) Design and synthesis of highly potent benzodiazepine gamma-secretase inhibitors: preparation of (2S,3R)-3-(3,4-difluorophenyl)-2-(4-fluorophenyl)-4-hydroxy-N-((3S)-1-methyl-2-oxo-5-phenyl-2,3-dihydro-1H-benzo[e][1,4]-diazepin-3-yl)butyramide by use of an asymmetric Ireland-Claisen rearrangement, *J. Med. Chem. 46*, 2275−2278.

26. Cheng, H. T., Miner, J. H., Lin, M., Tansey, M. G., Roth, K., and Kopan, R. (2003) Gamma-secretase activity is dispensable for mesenchyme-to-epithelium transition but required for podocyte and proximal tubule formation in developing mouse kidney, *Development 130*, 5031−5042.
27. De Strooper, B. (2003) Aph-1, Pen-2, and Nicastrin with Presenilin Generate an Active gamma-Secretase Complex, *Neuron 38*, 9−12.
28. Kang, D. E., Soriano, S., Xia, X., Eberhart, C. G., De Strooper, B., Zheng, H., and Koo, E. H. (2002) Presenilin couples the paired phosphorylation of beta-catenin independent of axin: implications for beta-catenin activation in tumorigenesis, *Cell 110*, 751−762.
29. Nicolas, M., Wolfer, A., Raj, K., Kummer, J. A., Mill, P., van Noort, M., Hui, C. C., Clevers, H., Dotto, G. P., and Radtke, F. (2003) Notch1 functions as a tumor suppressor in mouse skin, *Nat. Genet. 33*, 416−421.

BI049826U